Diffraction methods of drop size measurement in polydispersive media

TADEUSZ A. OPARA

Institute of Aviation Technology, Military University of Technology, ul. Kaliskiego 2, 00−908 Warszawa, Poland.

The principles of the diffractive method of drop size determination in the aerosol stream of fuel of significant diversification of drop dimensions are presented. Three variants of data processing obtained from the light intensity distribution $I(r)$ in the image plane are described. A comparison of both properties and applicability of the two variants is made.

1. Introduction

Conventional diffractometry is reduced to dimensional analysis of either monodispersive or quasi-monodispersive media while the position of the diffraction rings in the image plane is the source of information about the sizes of the light diffracting objects.

However, all these diffraction rings vanish for the drop pulverization spectrum $\rho(D)$ the relative standard deviation of which $(d = \sigma/\bar{D})$ exceeds the value $d_q = 0.153$ and thus it is no longer possible to estimate the average drop diameters $\bar{D}_\rho$.

The aerosol for which $d \geqslant d_q$ has the properties of polidyspersive medium and the information about sizes of its drops should be sought in other fragments of the diffraction image.

The value d_q denotes the relative standard deviation of the drop pulverization spectrum $\rho(D)$ for which the light intensity $I(r)$ is a monotonically decreasing function, in other words, $dI(r)/dr < 0$, in its whole domain. This function is only slightly dependent on the function describing the statistical distribution of the drop sizes in the stream of pulverized liquid.

In practice, the possibility of position determination for extrema of light intensity $I(r)$ disappears for the limiting value of the relative standard deviation $d_g \approx 0.12$ (for the case of direct recording of the $I(r)$ distribution) due to a significant decrease of contrast between them. The identification of the Airy fringes in diffractograms of $I(r)$ obtained by the indirect methods (photographic ones, for instance) is possible within the range $d = 0 - 0.1$.

The aerosol produced by turbine engine pulverizers, conventional carburettors, and low-pressure injectors of the fuel in piston OZI engines (of spark ignition) is a typical polydispersive medium. For this reason a conventional variant of the

method can be exploited only sporadically when the spread of drop sizes in a pulverized stream is small.

2. Comparison of the diffraction images of the monodispersive and polydispersive media

The light intensity $I_F(f,r)$, after the light wave passed through the aerosol stream being next Fourier transformed by the objective of focal length f, is a sum of images $I_F(D,f,r)$ produced by each of the illuminated drops

$$I_F(f,r) = \int_0^\infty \rho(D) I_F(D,f,r) \, dD. \tag{1}$$

The above expression constitutes the basis of integral methods for measuring drop diameters [1] − [7].

The parameter describing in a quantitative way the difference between the monodispersive and polydisperive media is the relative standard deviation $d = \sigma/\bar{D}_p$.

The statistical distributions of the same type but of diversified average drop diameters $\bar{D}_p$, while their value d is the same, produce similar diffraction images $I_F(f,r)$ differing only by the magnitude of characterstic parameters (half-width, diffraction interval and the like). After introducing the dimensionless optical Airy unit $z = (\pi \bar{D}_G r/\lambda)$ and normalizing the light intensity to the value $I_\rho(z)|_{z\to 0} = 1$ they become identical.
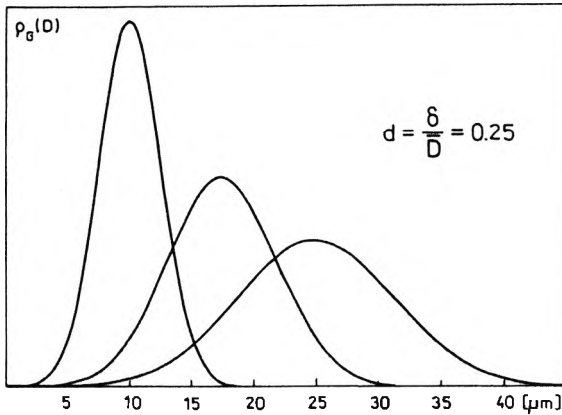

Fig. 1. Three Gaussian distributions $\rho_G(D, d)$ of different average diameters $\bar{D}_G$ (10, 17.5 and 25 μm) and the relative standard deviation $d = 0.25$ giving the same dimensionless diffraction image $I_G(z)$.

In Figure 1, three Gaussian distributions $\rho_G(D,d)$ of different average values $\bar{D}_g$ (10, 17.5 and 25 μm) and identical relative standard deviation $d = 0.25$ are presented, all giving the same diffraction image $I_G(z)$ (for the latter, see Fig. 2).
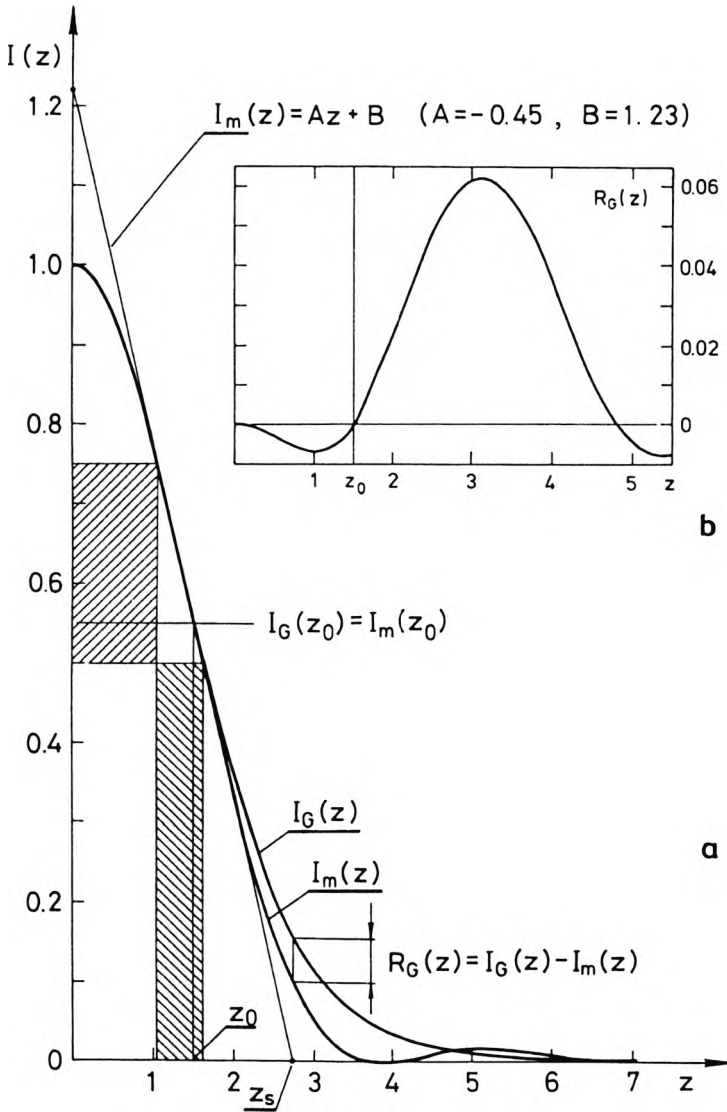
Fig. 2. Light intensity $I_G(z)$ for aerosol drop sizes whose are described by Gaussian distribution $\rho_G(D, d)$ of relative standard deviation $d = 0.25$ and the light intensity $I_m(z)$ for the monodispersive medium (a). Difference $R_G(z)$ between the light intensities $I_G(z)$ and $I_m(z)$ (b).

Diffraction image $I_G(z)$ is presented together with dimensionless intensity $I_m(z)$ of the light diffracted by the drops of the monodispersive medium of diameter $D_m = \bar{D}_G$.

Within the interval $z = 0 - 1.5$, the distributions $I_G(z)$ and $I_m(z)$ are almost identical while $I_G(z)$ is slightly less than $I_m(z)$. For the coordinate range $z = 1.5 - 4.5$, the intensities $I_G(z)$ and $I_m(z)$ start to differ while $I_G(z) > I_m(z)$.

Figures 2b and 3 show the difference $R_G(z)$ between the intensity of the light passing through a polydispersive and monodispersive media for several values of the
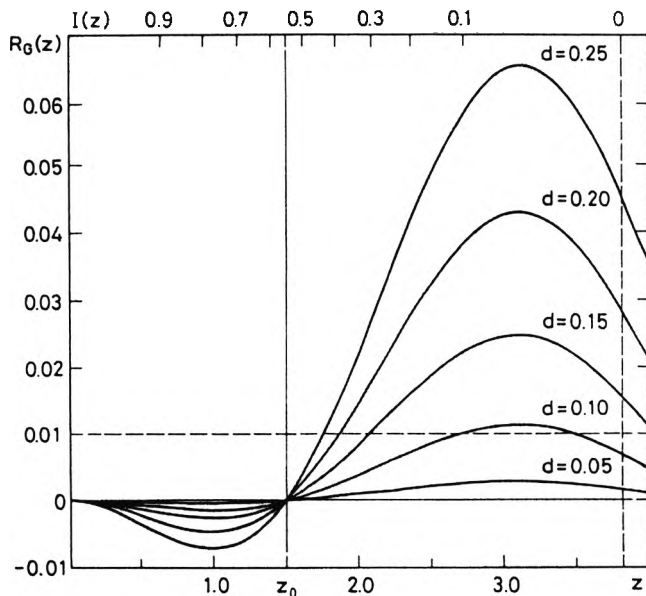
Fig. 3. Difference between the light intensities $I_G(z)$ and $I_m(z)$ as dependent on the relative standard deviation $d = \sigma/\bar{D}_G$.

relative standard deviation $d = \sigma/\bar{D}_G$

$$R_G(z) = I_G(z) - I_m(z). \tag{2}$$

This difference takes its extreme values for $z \approx 1$ and $z \approx 3$ while $R_G(z_0) \to 0$ for $z \approx 1.5$ independently of the value d.

In paper [8], it has been stated that the kind of the function $\rho(D)$ describing the statistical distribution of the drop sizes in the aerosol stream has no essential influence on the light intensity $I_\rho(z)$ in the diffraction image. The results of the analysis carried out confirm this statement. For symmetric characteristics of pulverization $\rho(D)$ the functions of light intensity distribution $I_\rho(z)$ are practically indiscriminable within the range of $z = 0-2.5$. For nonsymmetric spectrum of the drop diameters $\rho(D)$ the character of changes of $R(z)$ functions is very similar except for its zero position which differs slightly from z_0.

In Figure 4, the functions $R(z)$ are shown for three distributions: normal $\rho_G(D)$, uniform $\rho_r(D)$ and logarithmic $\rho_l(D)$, all of the same value of the relative standard deviation $d = 0.25$:

$$\rho_G(D) = \frac{1}{\sigma\sqrt{2\pi}} \exp\left[-\frac{(D-\bar{D}_G)^2}{2\sigma}\right], \quad d_G = \frac{\sigma}{\bar{D}_G}, \tag{3}$$

$$\rho_l(D) = \frac{1}{\sigma D\sqrt{2\pi}} \exp\left[-\frac{(\ln D - m)^2}{2\sigma}\right], \quad d_l = \frac{\sqrt{\exp(2m+\sigma^2)(\exp\sigma^2 - 1)}}{\exp\left(m+\frac{\sigma^2}{2}\right)}, \tag{4}$$

$$\rho_r(D) = \frac{1}{2h} \quad \text{for} \quad (\bar{D}_r - h) < D < (\bar{D}_r + h), \quad d_r = \frac{h}{\sqrt{3\bar{D}_r}}. \tag{5}$$

The influence of the type of statistical distribution function $\rho(D)$ on the difference value $R_\rho(z) = I_\rho(z) - I_m(z)$ starts to be visible first for the dimensionless coordinate $z > 2.5$.
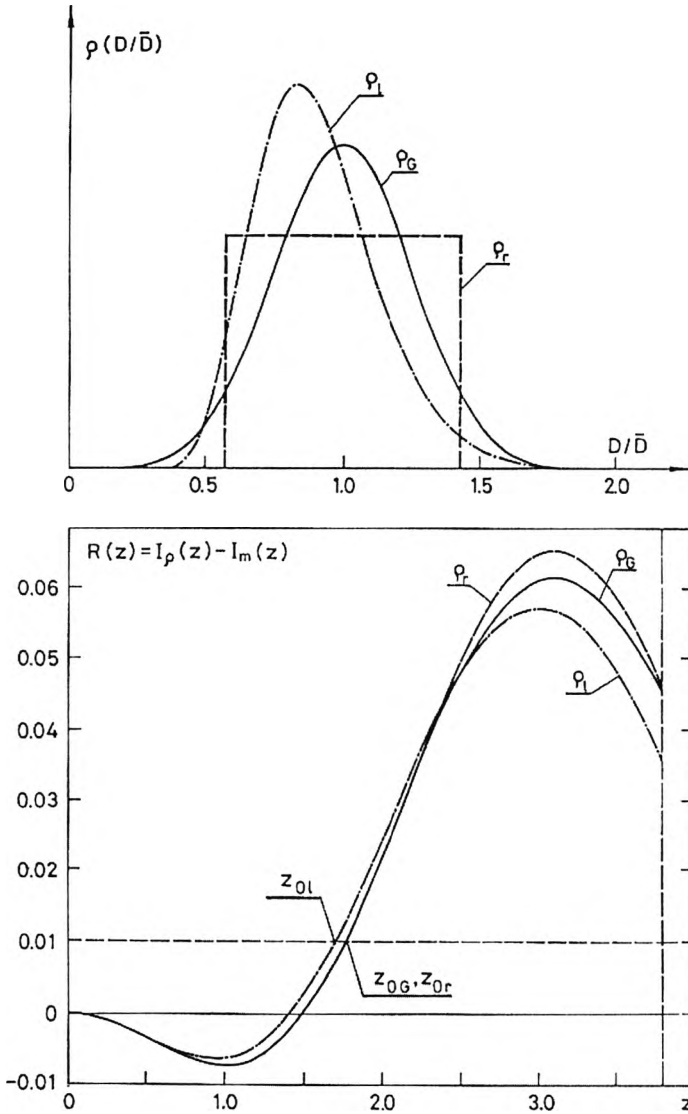

Fig. 4. Three statistical distributions of the drop sizes $\rho(D)$ in the media of the same average diameter $\bar{D}_\rho$ and the same relative standard deviation $d = 0.25$ as well as the corresponding functions $R_\rho(z) = I_\rho(z) - I_m(z)$ ($\rho_l(D)$ — logarithmic distribution, $\rho_G(D)$ — Gaussian distribution, $\rho_r(D)$ — uniform distribution).

The basic conclusion from this analysis is the statement that the dimensionless function describing the light intensity distribution in the diffraction image $I(z)$ in the range of $z = 0 - 1.6$ ($I(z) = 1 - 0.5$) contains information about the average value of $\bar{D}_p$ of the statistical distribution $\rho(D)$ of the drop sizes in the aerosol stream. Even for very great values of the relative standard deviation d the maximal difference $|R(z)|$ is less than 0.01 within this range (Fig. 3).

3. Calculation of the average drop diameter $\bar{D}_p$ based on linear approximation of $I(z)$ function

For dimensionless coordinate $z = 1.1 - 1.6$ (hatched area in Fig. 2) the function $I_m(z)$ has a quasi-linear character and can be approximated as follows:

$$I_m(z) \simeq I_{ml}(z) = Az + B = A\frac{\pi D_m r}{\lambda f} + B, \quad (A = -0.45, \ B = 1.23). \tag{6}$$

The linear coefficient of this approximation amounts to $r_m = -0.99993$. Using the r.m.s. method to minimize the difference S between the light intensity $I(r)$ determined experimentally and the straight line $I_{ml}(z)$ for k experimental points of $I(r_i)$ we get

$$S = \sum_{i=1}^{k} \left[\frac{I(r_i)}{I_{\max}} - \left(A\frac{\pi D_m}{\lambda f}r_i - B \right) \right]^2, \quad I_{\max} = I_F(f,r)|_{r \to 0}, \tag{7}$$

and the drop diameter D_m is calculated from the relation

$$D_m = \frac{\dfrac{1}{I_{\max}} \sum\limits_{i=1}^{k} r_i I(r_i) - B \sum\limits_{i=1}^{k} r_i}{\dfrac{A\pi}{\lambda f} \sum\limits_{i=1}^{k} r_i}. \tag{8}$$

The value of D_m determined in this way is a magnitude of the drops in the dimensionally uniform medium the diffraction image of which is closer to the real course of the function describing the light intensity distribution $I(r)$ in the polydispersive medium of pulverization spectrum $\rho(D)$. Thus, it can be assumed that

$$\bar{D}_p \simeq D_m. \tag{9}$$

The simulation calculations carried out for different statistical distributions $\rho(D)$ showed that the entire systematic error caused by applying the approximations (6) and (9) is less than 1%.

In the method described only 1/4 of the information contained in the recorded light intensity distribution $I(r)$ is exploited since the range within which the linearization of $I_m(z)$ was performed (*i.e.*, $z = 1.1 - 1.6$) corresponds to the range $(0.5 - 0.75)I_{\max}$.

Using relation (8) in order to calculate the average diameter $\bar{D}_p \simeq D_m$ of the drops allows us to obtain results of relatively small random error since in this part of

the distribution $I(r)$ the changes in the light intensity are most pronounced for advantageous signal-to-noise ratio. This follows from the fact that the derivative of the light intensity $dI(r)/dr$ reaches its maximal value within this range. For a monodispersive medium the extremal value of $dI_m(z)/dz = -0.46$ (for $z = 1.49$, $I(z) = 0.56$) while the tangent at this point described by equation

$$I'_m(z) = -0.46z + 1.24 \qquad (10)$$

differs slightly from the line $I_{ml}(z) = -0.45z + 1.23$ approximating the relation $I_m(z)$. For the polydispersive media the maximal value of the derivative modulus $|dI_\rho(z)/dz|$ diminishes which causes that the lines $I'_\rho(z)$ and $I_{ml}(z)$ practically cover each other. This observation can be exploited for graphical method of diffractogram elaboration allowing us to obtain quickly some preliminary results of measurements.

Drawing a tangent to the curve $I(r)$ from the point $(0, 1.23 I_{max})$ the value r_s is determined at the point of intersection with the horizontal axis. Substituting this value to the relation for the zero position $z_s = 2.73$ of the line $I_{ml}(z)$, (Fig. 2) we obtain

$$\bar{D}_\rho \simeq D_m = 0.87 \, \frac{\lambda f}{r_s}. \qquad (11)$$

It is possible to use formulae (8) and (11) only when the absolute values of the light intensity distribution $I(r)$ in the diffraction image are known.

The direct recording of the diffraction images (scanning of the chosen area with a single photodetector or using the mosaic systems composed of a large number of detectors) is difficult in technical implementation because of disadvantageous relation between the useful signal $I_F(f, r)$ and the useless one $I_0(r)$. The knowledge of the distribution $I(r) = I_F(f, r) + I_0(f, r)$ creates a possibility of determining the average diameter of the aerosol drops with the least random error.

4. Photographic recording of diffraction image

In the Fourier transformation of the light beam propationg through the stream examined the diffraction part of the light intensity $I_F(f, r)$ constitutes only a "background" for the image of the plane wave focus since $I_0(r)|_{r \to 0} \gg I_F(r)|_{r \to 0}$. The photographic recording of the diffraction image allows us to reduce the difficulties which appear in the course of direct measurement of the distribution $I(r)$. If the exposure conditions are properly chosen its maximal value $I_{F max} = I_F(r)|_{r \to 0}$ should be located in the upper part of the linear range of the Hurter–Driffield curve [9], [10], Fig. 5, defining the relation between the light intensity and the optical density (blackening) of the photographic emulsion.

A microdensitogram of the diffraction image $\Phi(r)$ allows us to determine the distribution $I'(r)$ which after taking account of the value $I_A + \Delta$ is proportional to the real distribution of the light intensity $I(r)$

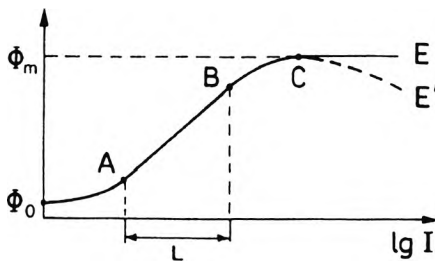$$I(r) = (I_A + \Delta) + I'(r). \qquad (12)$$

Fig. 5. Exposure curve for the photographic materials (AB — linear range, CE' — solarization range).

The value I_A determined from the photochemical characteristics $\Phi = \Phi(\log I)$ of the light sensitive material used should be corrected due to the fact that the final effect of the photographic recording (in the form of blackening) depends to a high degree on the photochemical processing parameters of the negative. For this reason the correction Δ should be taken into account in relation (12) which can be determined from the sensitometric measurements or be treated as a second unknown. Then relation (7) takes the form

$$S = \sum_{i=1}^{k} \left[\frac{(I_A + \Delta) + I'(r_i)}{(I + \Delta) + I'_{max}} - \left(A \frac{\pi D_m}{\lambda f} r_i - B \right) \right]^2. \tag{13}$$

Applying the formalism of the r.m.s. method with unknown D_m and Δ leads to a system of nonlinear equations. Using the approximation

$$\frac{(I_A + \Delta) + I'(r_i)}{(I_A + \Delta) + I'_{max}} \simeq \frac{(I_A + I'_{max}) + \Delta [I'_{max} - I'(r_i)]}{(I_A + I'_{max})^2} \tag{14}$$

a set of linear equations is obtained from which the values D_m and Δ were determined

$$\bar{D}_\rho \simeq D_m = \frac{B(I'_{max} + I_A)(F_1 F_6 - F_0 F_2) + F_2 F_3 - F_1 F_4}{\dfrac{A\pi(I'_{max} + I_A)}{\lambda f} F_2^2 - F_1 F_5}, \tag{15}$$

$$\Delta = \frac{(I'_{max} + I_A)[B(I'_{max} + I_A)(F_2 F_6 - F_0 F_5) + F_3 F_5 - F_2 F_4]}{F_2^2 - F_1 F_5}. \tag{16}$$

The coefficients F_i occurring in the above equations are calculated from the relations:

$$F_0 = \sum_{i=1}^{k} [I'_{max} - I'(r_i)], \qquad F_1 = \sum_{i=1}^{k} [I'_{max} - I'(r_i)]^2,$$

$$F_2 = \sum_{i=1}^{k} [I'_{max} - I'(r_i)] r_i, \qquad F_3 = \sum_{i=1}^{k} [I'_{max} - I'(r_i)][I'(r_i) + I_A],$$

$$F_4 = \sum_{i=1}^{k} r_i I'(r_i), \qquad F_5 = \sum_{i=1}^{k} r_i^2, \qquad F_6 = \sum_{i=1}^{k} r_i. \tag{17}$$

Approximation (14) is well fulfilled if the correction parameter $\Delta \leqslant 0.2 I_A$. The determination accuracy of the average drop diameter $\bar{D}_\rho$ improves while serial measurements are performed (recorded on the same film) since for all the microdensitograms the same averaged value $\bar{\Delta}$ is assumed.
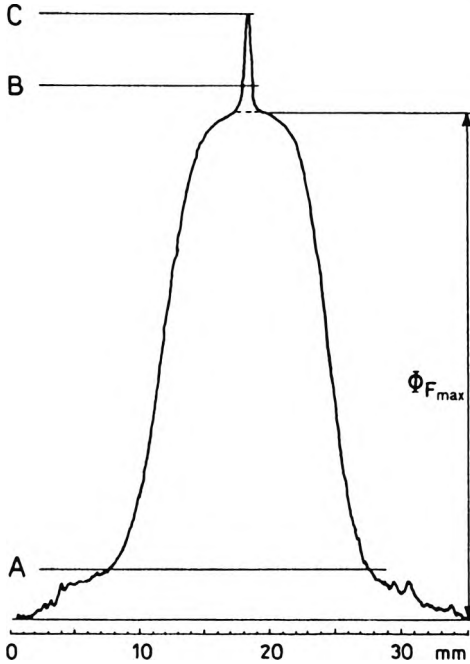

Fig. 6. Microdensitogram $\Phi(r)$ of the diffraction image appearing after the light wave has passed through the pulverization cone of the injector of 16.83.0310 type of the GTD-350 engine under the fuel forcing pressure $p = 1.0$ MPa.

In Figure 6, a microdensitogram of the diffraction image recorded after a light wave of wavelength $\lambda = 0.63$ μm has passed through the pulverization cone of the fuel injector of 16.83.0310 type of GTD-350 engine is presented. The photographic recording (exposure time 1/125 s) was realized using the Gold 200 negative which was developed in the C-41 process. In order to measure the optical density $\Phi(r)$ an automatic microdensitometer of MD 100 type was used. The average drop diameter calculated from relation (15) appeared to be equal to $\bar{D}_\rho = 30 \pm 2$ μm.

The photographic recording of the diffractive image is relatively simple to realize. The advantages offered by this method are short time of measurement and easiness of storing the experimental data. The basic disadvantage of the method is the necessity of labour-consuming microdensitometric processing as well as an increase of the random error of measurements characteristic of each indirect method of information processing.

During the preliminary measurements the photographic recording of the diffraction images was done by changing the exposure time as well as both sensitivity

and type of the negative materials. No distinct influence of either the type of light sensitive materials used or the photochemical processing parameters on the average value of the drop diameter $\bar{D}_\rho$ determined from the analysis of the microdensitogram $\Phi(r)$ has been observed. However, the accuracy and repeatability of the measurements is, in an indirect way, dependent on the photographic recording quality, *i.e.*, on the contrast, level of smoke and the sizes of grains.

The best results have been obtained when exploiting the light sensitive materials applied in holography. The majority of measurements (some hundreds of them) were carried out using the Gold 200 negatives developed according to C-41 process. The correction parameter Δ calculated from Eq. (16) or determined from sensitometric measurements was contained in the $(0.05 - 0.10)I_A$ range. For preliminary measurements it may be assumed that $I(r) \approx I'(r) + I_A$ and in order to determine the diameter $\bar{D}_\rho$ the much simpler calculation formula (8) can be used.

From the three variants of quasi-linear fragment of light intensity distribution $I_m(r)$ the most important and most general is the last one (relations (15) and (16)) connected with the photographic recording of the diffraction image. This renders it possible to determine the average drop diameter $\bar{D}_\rho$, independent of the type of function describing the pulverization spectrum $\rho(D)$ of the aerosol and the value of the relative standard deviation d.

5. Linear transformation method for the light intensity distribution $I(r)$

When using the photographic recording the light intensity distribution $I(r)$ in the focal plane of the objective is reconstructed from a microdensitogram $\Phi(r)$. The linear approximation of the quasi-linear fragment of the function $I(r)$ allows us to calculate the average diameter $\bar{D}_\rho$ of the aerosol drops in the stream. In this way the range $(0.50 - 0.75)I_{F\max}$ is exploited which constitutes only as much as 1/4 of the information contained in the diffractogram.

Expanding this range makes it possible to determine the diameter $\bar{D}_\rho$ with better accuracy and obtain additional information about the pulverization spectrum $\rho(D)$ of the aerosol drops [11].

The dimensionless function $\Lambda_{wm}(z)$ describing the intensity distribution of the light diffracted in the monodispersive medium can be used as a standard with which the real light intensity distrbution $I_w(r) = I(r)/I_{F\max}$ is compared. The essence of the linear transformation is to find the correlation between the dimensionless coordinate z of the distribution $\Lambda_{wm}(z_i)$ and the radius vector r_i in the diffraction image

$$\Lambda_{wm}(z_i) = I_w(r_i) \rightarrow z_i = \frac{\pi}{\lambda f} D r_i. \tag{18}$$

For the monodispersive aerosol the correlation function $z = t_m(r)$ is of linear character (Fig. 7a), therefore for k points (r_i, z_i) we have

$$D_m = \frac{\lambda f}{k\pi} \sum_{i=1}^{k} \frac{z_i}{r_i} = \frac{\lambda f}{\pi} \tan \gamma. \tag{19}$$
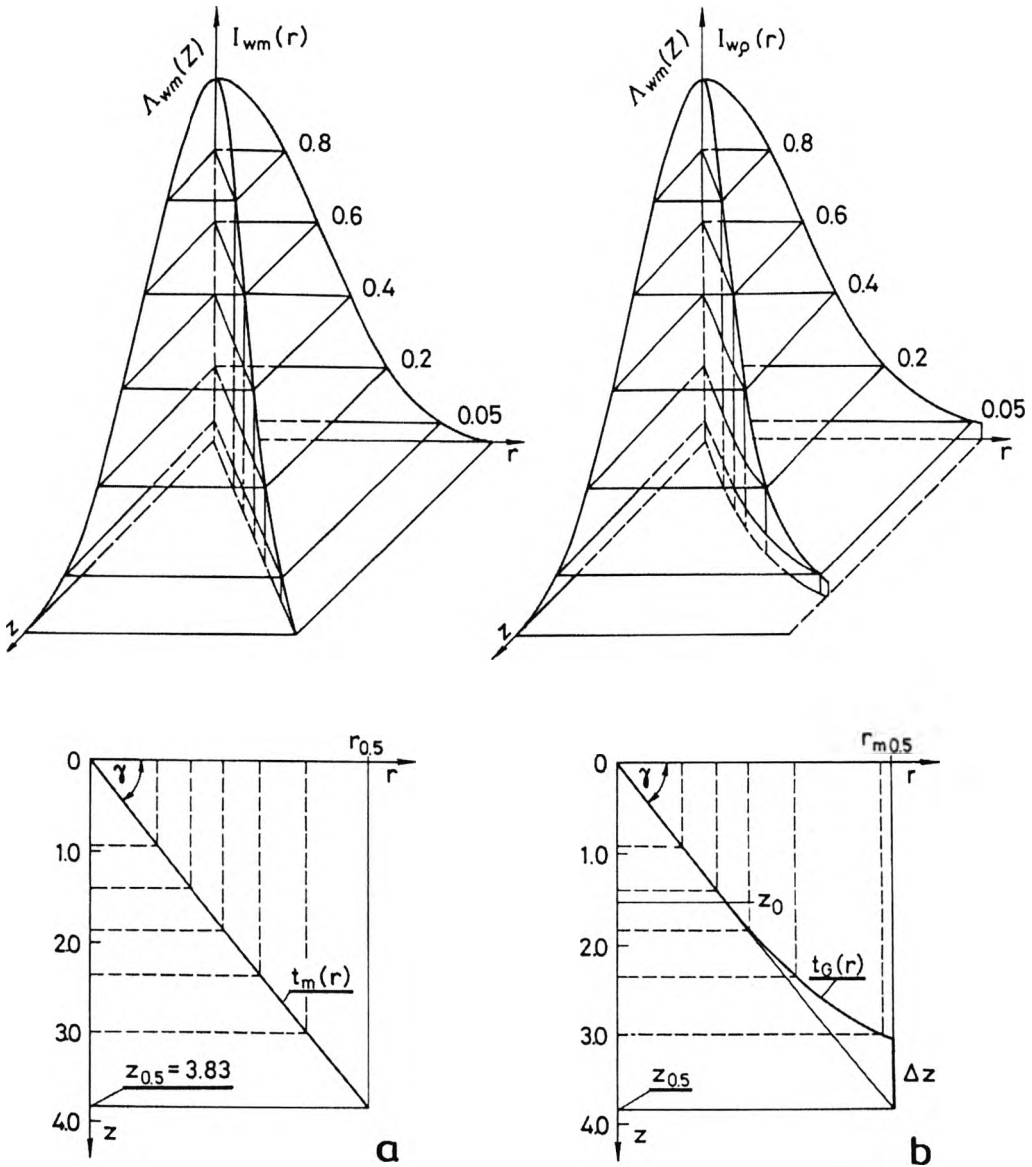
Fig. 7. Scheme illustrating the transformation principle for the relation $I_{wp}(r) = I_p(r)/I_{p\,max}$ describing the light intensity distribution in the diffraction image (a — monodispersive medium, b — polydispersive medium as described by Gaussian distribution $\rho_G(D)$ of relative standard deviation $d = \sigma/\bar{D}_G = 0.25$).

The pulverized stream of liquid having features of a polydispersive medium produces the diffraction image $I_{wp}(r)$ of which the transform $z = t(r)$ is no more a linear function. This is illustrated in Fig. 7b, where the relation $z = t_G(r)$ is presented for the stream whose drop sizes are described by the Gauss distribution of relative standard deviation $d = \sigma/\bar{D}_G = 0.25$.

T a b l e 1. Dimensionless function $I(z)$ describing the intensity distribution of the light diffracted in the monodispersive medium.

$I(z)$	z	$I(z)$	z	$I(z)$	z	$I(z)$	z
0.99	0.2004	0.74	1.0836	0.49	1.6383	0.24	2.2432
0.98	0.2840	0.73	1.1072	0.48	1.6603	0.23	2.2719
0.97	0.3486	0.72	1.1305	0.47	1.6823	0.22	2.3011
0.96	0.4034	0.71	1.1536	0.46	1.7045	0.21	2.3311
0.95	0.4520	0.70	1.1766	0.45	1.7268	0.20	2.3618
0.94	0.4962	0.69	1.1993	0.44	1.7491	0.19	2.3933
0.93	0.5371	0.68	1.2219	0.43	1.7716	0.18	2.4257
0.92	0.5755	0.67	1.2444	0.42	1.7943	0.17	2.4591
0.91	0.6118	0.66	1.2667	0.41	1.8171	0.16	2.4935
0.90	0.6463	0.65	1.2889	0.40	1.8400	0.15	2.5291
0.89	0.6794	0.64	1.3110	0.39	1.8631	0.14	2.5661
0.88	0.7113	0.63	1.3330	0.38	1.8865	0.13	2.6046
0.87	0.7420	0.62	1.3550	0.37	1.9100	0.12	2.6448
0.86	0.7718	0.61	1.3769	0.36	1.9337	0.11	2.6869
0.85	0.8008	0.60	1.3987	0.35	1.9577	0.10	2.7314
0.84	0.8290	0.59	1.4205	0.34	1.9819	0.09	2.7785
0.83	0.8566	0.58	1.4422	0.33	2.0064	0.08	2.8288
0.82	0.8336	0.57	1.4640	0.32	2.0312	0.07	2.8831
0.81	0.9100	0.56	1.4857	0.31	2.0563	0.06	2.9421
0.80	0.9359	0.55	1.5074	0.30	2.0818	0.05	3.0075
0.79	0.6914	0.54	1.5291	0.29	2.1076	0.04	3.0814
0.78	0.9865	0.53	1.5509	0.28	2.1338	0.03	3.1576
0.77	1.0113	0.52	1.5727	0.27	2.1604	0.02	3.2736
0.76	1.0357	0.51	1.5945	0.26	2.1875	0.01	3.4197
0.75	1.0598	0.50	1.6163	0.25	2.2151	0.00	3.8317

A comparison of the function $\Lambda_{wm}(z)$ and $I_w(r)$ can be carried out in the range within which these functions are monotonic. To this end, the data from Tab. 1 are used, where the dimensionless coordinates z_i for consecutive values $\Lambda_{wm}(z_i)$ changing with a steady step from unity to zero are presented.
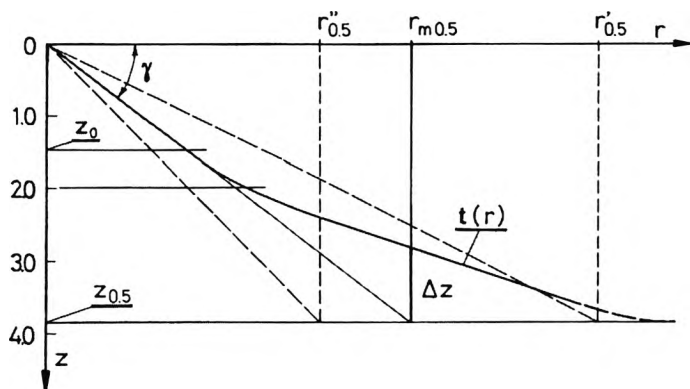

Fig. 8. Transform $t(r)$ of the diffraction image of the medium in which there appears the equal number of drops of sizes $D' = D$ and $D'' = 2D$.

For coordinate $z \leqslant 2$ the transform $z = t(r)$ is of quasi-linear character, independent of the type of statistical distribution $p(D)$ and the value of the relative standard deviation d. If the dark and bright rings are visible in the diffraction image (quasi-monodispersive medium) the function $z = t_{qm}(r)$ ends at the point $r_{0.5}$ (Fig. 9).
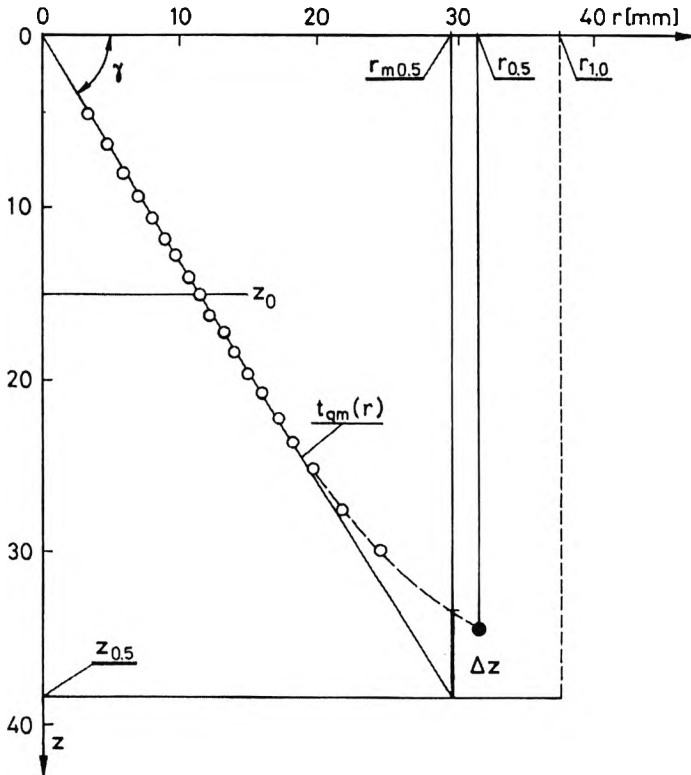

Fig. 9. Transform t_{qm} of the diffraction image of the pulverization cone of the starting injector of K 108-767 type at the pressure of fuel forcing equal to $p_t = 1.0$ MPa.

For a polydispersive medium the relation $z = t_p(r)$ tends asymptotically to the line $z = 3.832$ corresponding to the first extremum of the standard function $\Lambda_{wm}(z)$, Fig. 10.

A comparison of the transforms $t_m(r)$ and $t_p(r)$, i.e., the ones for uniform aerosols and those dimensionally diversified but fulfilling the condition $\bar{D}_p = D_m$, leads to the same conclusions which have been formulated for the relation $R(z) = I_p(z) - I_m(z)$. At the point z_0 being the zero position of the function $R(z)$ the transforms $t_p(r)$ and $t_m(r)$ intersect each other (Figs. 8 – 10).

Calculating the average drop diameter $\bar{D}_p$ from relation (19) for a quasi-monodispersive medium the transform $t_{qm}(r)$ can be used in the whole range since the systematic error caused by its nonlinearity will be less than 1%.

For the polydispersive media the deviations from linearity of the function $t_p(r)$ are significant (Fig. 7). For that reason, when calculating the diameter $\bar{D}_p$ from
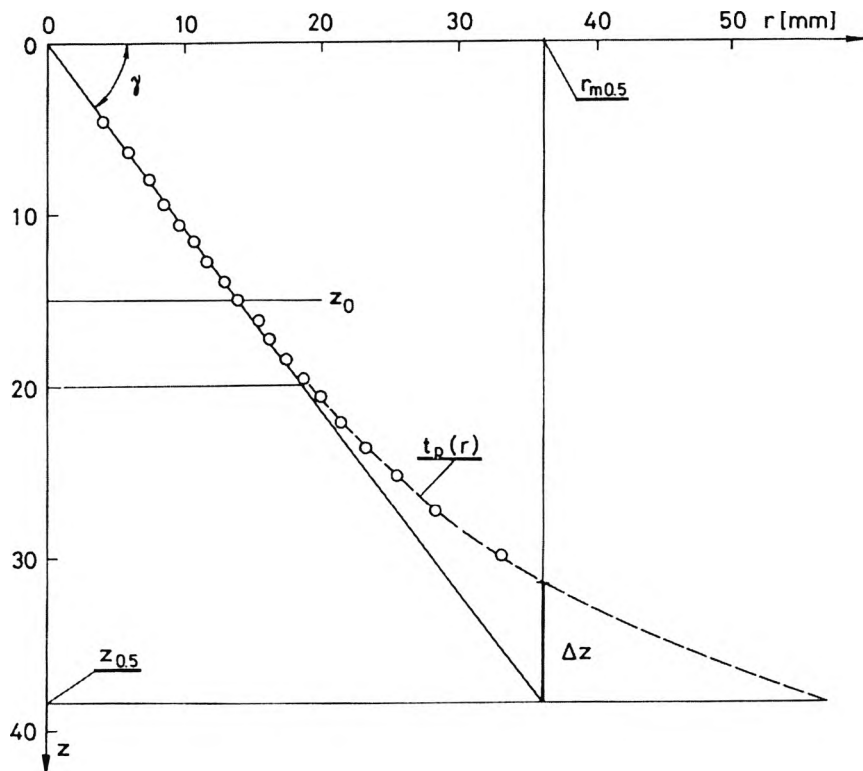
Fig. 10. Transform $t_p(r)$ of the diffraction image created by the pulverisation cone of the main injector of K 108-767 type at the fuel forcing pressure $p_t = 10$ MPA.

relation (19) the points from the linear fragment of transform $t_p(r)$, i.e., those from the range $z = 0-2$ ($I_w(r) = 0.33-1.0$), should be taken into account. Thus, the straight line

$$z = \frac{\pi}{\lambda f} \bar{D}_\rho r = \frac{\pi}{\lambda f} D_m r = r \tan \gamma \qquad (20)$$

is the transform of the light intensity distribution $I_m(r)$ for a monodispersive aerosol whose drop sizes D_m correspond to average value $\bar{D}_\rho$ of the pulverization spectrum.

The point of intersection of the line $z = D_m r = \bar{D}_\rho r$ with the straight line $z = z_{0.5} = 3.832$ determines the position of the first dark ring $r_{m0.5}$ of the distribution $I_m(r)$ which is statistically equivalent to the real distribution $I_w(r) = I(r)/I_{F\max}$. This means that for k points constituting the basis for calculating the value $\bar{D}_\rho$ the sum

$$S = \sum_{i=1}^{k} [I_w(r_i) - I_m(r_i)]^2. \qquad (21)$$

takes its minimum.

The shape of transform $t(r)$ is characteristic of the type of the drop size distribution $\rho(D)$. In Figure 6, the function $t(r)$ is shown for the medium in which

one half of the drops have $D' = D$ diameter while the other half satisfies $D'' = 2D$. The average value calculated from relation (19) for the points from the range $z = 0-2$ is $\bar{D} = 1.486D$ and remains (within the limits of the assumed error) consistent with the average $\bar{D} = 1.5D$ $((\bar{D}-D)/\bar{D} = 0.9\%)$. The transform $t(r)$ distinctly "breaks" into two rectilinear fragments (ranges: $z = 0-2$ and $z = 2-z_{0.5}$) of different slope while the derivative $dt(r)/dr$ has a characteristic "stepped" shape.

For monodispersive media the slope of the $t_m(r)$ line is invariably of the form

$$\frac{dt_m(r)}{dr} = \text{idem} = \tan \gamma = \frac{z_{0.5}}{r_{0.5}} = \frac{3.832}{r_{0.5}} = \frac{\pi}{\lambda f} D_m. \tag{22}$$

The derivatve $dt_m(r)/dr$ is almost constant for the quasi-monodispersive aerosols. For the radius vector r to $r_{0.5}$ close its value is slightly smaller (Fig. 9).

In the stream of liquid of diversified drop sizes the derivative $dt_p(r)/dt$ is approximately constant only in this fragment of the transform in which $t_p(r) \leqslant 2$ (Fig. 10). In the further part its value diminishes gradually.

The difference between the respective transforms $t_m(r)$ and $t_p(r)$ of the monodispersive and polydispersive media can be determined qualitatively in a most convenient way for the coordinate $r_{m0.5}$ (Figs. 7-10) as

$$\Delta z = z_{0.5} - t(r_{m0.5}) = 3.832 - t(r_{m0.5}). \tag{23}$$

The value of Δz permits to estimate the relative standard deviation $d = \sigma/\bar{D}_p$ of the scattering characteristics $\rho(D)$.

In Figures 9 and 10, the transforms $t_{qm}(r)$ and $t_p(r)$ of the diffraction images created due to passage of the light wave through the pulverization cones of the injectors applied in the Lis-5 engines are presented.

At the pressure of fuel forcing $p_t = 4.5$ MPa the main injector of the K 108-012 type produces a drop stream of significantly differentiated diameters. The diffractive image $I(r)$ is of monotonic character while its transform for $t_p > 2$ tends asymptotically to the value $z = 3.832$. The average diameter of the drops is calculated for thirteen points (Fig. 10) of $I(r)$ equal to: 0.05, 0.10, ..., 0.65 takes the value $\bar{D}_p = 21.7$ μm ($\Delta z = 0.7$).

The method of linear transformation allows us to calculate the average diameter $\bar{D}_p$ of the aerosol drops to the relatively high accuracy. This follows from the fact that the data contained in the light intensity distribution $I(r)$ are exploited in a wider range. For the polydispersive media $(0.33-1.0)I_{F\,max}$ while for those of dimensional uniformity $(0.0-1.0)I_{F\,max}$ Also, it is estimated that, when calculating the value of $\tan\gamma$, the greatest statistical weight is attributed to the points from the central fragment of the $I_w(r)$ function which are characterized by an advantageous signal-to-noise ratio any by position in the region in which the influence of the diffractive background $I_0(r)$ is minimal.

6. Conversion of the diffraction image

The function $R_\rho(z) = I_\rho(z) - I_m(z)$ illustrating the difference between the light intensity in the diffraction images of the beam of drops of pulverization spectrum
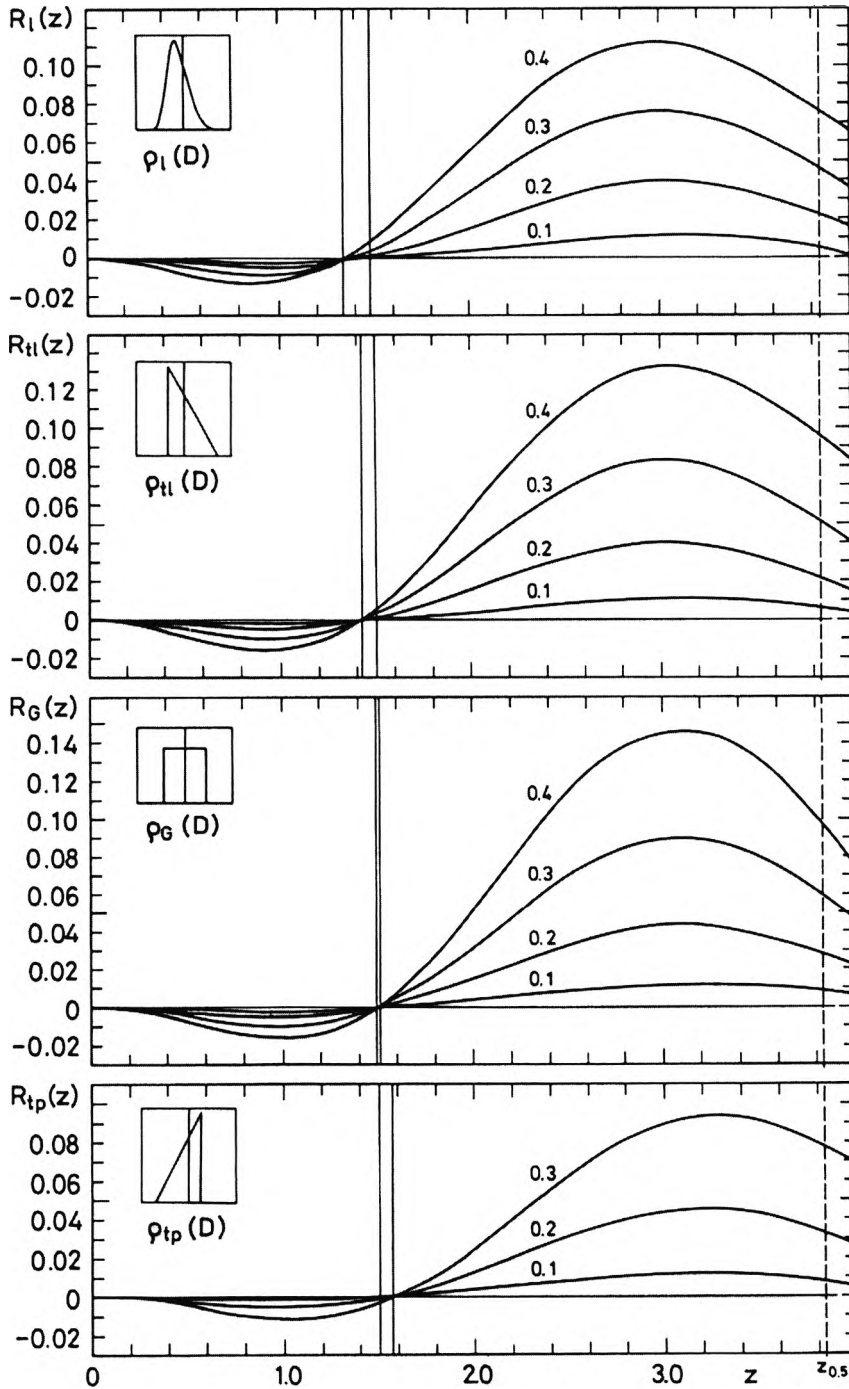
Fig. 11. Functions $R_\rho(z) = I_\rho(z) - I_\rho(z)$ for statistical distributions $\rho(D)$; ($\rho_l(D)$ — logarithmic normal distribution, $\rho_{tl}(D)$ — triangular distribution ($\gamma > 0$), $\rho_r(D)$ — uniform distribution, $\rho_{tp}(D)$ — triangular distribution ($\gamma < 0$)).

$\rho(D)$ and that of monodispersive medium of drops dimensionally uniform takes a zero value, *i.e.*, $R_\rho(z) = 0$. The position of the z_0 point at which $I_\rho(z) = I_m(z)$ depends on the kind of drop pulverization spectrum $\rho(D)$ as well as on the relative standard deviation d (Fig. 11).

In Figure 11, the relation $z_0(d)$ is shown for the Gaussian distribution $\rho_G(D)$, uniform distribution $\rho_r(D)$, logarithmic $\rho_l(D)$ and two triangular distributions $\rho_{tl}(D)$ and $\rho_{tp}(D)$ of opposite asymmetry coefficients γ [12].

The position of the point z_0 changes to the least degree when the pulverization spectrum is symmetric.

The lines $z_0(d)$ for the nonuniform and Gaussian distributions have the common origin $z_0(0) = 1.49$ and the maximal difference between them does not exceed 0.5%. The point $z_0(0) = 1.49$ is characteristic of all symmetric distributions and the corresponding relations $z_0(d)$ have almost identical quasi-linear shape as that for functions $\rho_r(D)$ and $\rho_G(D)$.

For the pulverization spectrum $\rho(D)$ of positive coefficient of asymmetry $\gamma > 0$ ($\rho_l(D)$ and $\rho_{tl}(D)$) the relations $z_0(d)$ diminish in a monotonic way. On the other hand, if $\gamma < 0$ ($\rho_{tp}(D)$) the function $z_0(d)$ is of increasing character (Fig. 12).
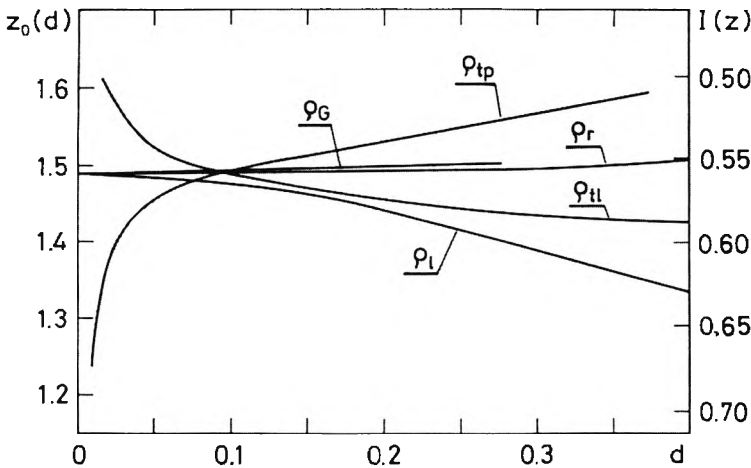

Fig. 12. Dependence of the zero order place z_0 of the function $R_\rho(z)$ on the relative standard deviation d for five statistical distributions ($\rho_l(D)$ — logarithmic normal distribution, $\rho_{tl}(D)$ — triangular distribution ($\gamma > 0$), $\rho_G(D)$ — Gaussian distribution, $\rho_r(D)$ — uniform distribution, ρ_{pt} — triangular distribution ($\gamma < 0$)).

For the triangular distributions $\rho_{tl}(D)$ and $\rho_{tp}(D)$ of opposite coefficients γ the corresponding lines $z_0(d)$ show almost mirror reflection symmetry with respect to the zero places of the symmetric functions $\rho_r(D)$ and $\rho_G(D)$.

The position of the zero places $z_0(d)$ is least diversified for the relative standard deviation $d = 0.1$. Significant divergences among the values of $z_0(d)$ within the interval $d = 0-0.1$ have no significance since in this range the difference $R_\rho(z) = I_\rho(z) - I_m(z)$ is very small (Fig. 11).

For each type of pulverization spectrum $\rho(D)$ the zero place $z_{0\min}$ can be determined which corresponds to the minimum of the error parabola $S_\rho(z)$, Fig. 13,

$$S_\rho = \frac{1}{d_k} \int_0^{d_k} |R_\rho| dz. \tag{24}$$

The function $S_\rho(z)$ is a total integral average of the modulus of the difference $R_\rho(z)$ between the light intensity distribution $I_\rho(z)$ for a polydispersive medium and that for the monodispersive medium $I_m(z)$.

The essential problem is determination of the upper integration limit d_k, in other words, the maximal value of the relative standard deviation. In the case of the following distributions: $\rho_G(D)$, $\rho_{tp}(D)$, $\rho_r(D)$ and $\rho_{tl}(D)$ there exist a natural limit for the value of d which follows from the obvious fact that the diameter D of the

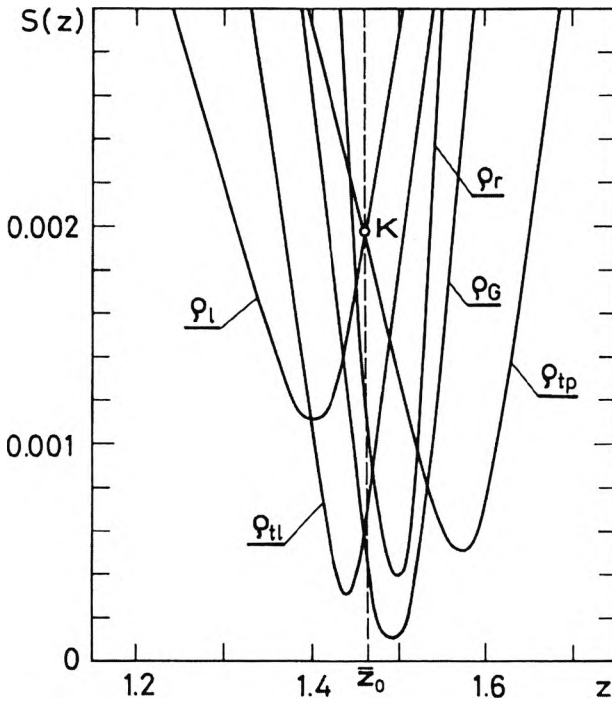

Fig. 13. Average value of the difference $S_\rho(z)$ for five statistical distributions $\rho(D)$, ($\rho_G(D)$ − Gaussian distribution, $\rho_r(D)$ − uniform distribution, $\rho_{tl}(D)$ − triangular distribution ($\gamma > 0$), $\rho_{tp}(D)$ − triangular distribution ($\gamma < 0$), $\rho_l(D)$ − logarithmic normal distribution).

drops must be a positive number. Hence, the physical meaning of the above functions will be preserved when $d_G \leqslant 0.30$, $d_{tp} \leqslant 0.35$, $d_r \leqslant 0.58$ and $d_{tl} \leqslant 0.71$.

The limitations of this kind do not occur for the equations applied most frequently to perform approximations of the real pulverization spectrum, i.e., $\rho_{RR}(D)$, (Rosin–Rammler), $\rho_{NT}(D)$, (Nukiyama–Tanasawa), and $\rho_l(D)$.

The fundamental property of the diffraction method consists in the fact that their sensitivity and selectivity are inversely proportional to the sizes of the drops

occurring in the light beam. This means that even in the case of the optimally chosen parameters of the optical system there exists a limiting value for the drop diameter D_g above which no measurable effect of changes in the light intensity distribution $I_F(r)$ can be recorded in the image plane. The value of D_g is determined experimentally taking account of the diffraction background.

Aberrations of the optical elements, diffraction and scattering of the light beam at all the pollutants existing in the measurement space as well as the light diffusion on the active surface of the detection systems cause a spread of the image at the point where the plane focuses. Assuming the half-width $2r_t$ of the distribution $I_0(r)$ as a measure of this spread a relation is obtained from which the values D_g can be estimated

$$D_g = \frac{z\left(\frac{1}{2}I_{F\max}\right)\lambda f}{\pi r_t} \simeq \frac{\lambda f}{2r_t}. \tag{25}$$

The drops of diameters $D > D_g$ produce the diffraction distributions which totally disappear in the focus image.

The maximal value of the relative standard deviation d_k for the pulverization spectrum $\rho(D)$ is defined in such a way that the quantitative contribution of the drops of diameters $D > D_g$ be not greater than 1%.

When calculating the function $S_\rho(z)$ the upper limit of integration $d_k = 0.40$ has been assumed. This is averaged value for typical statistical distributions ($\rho_i(D)$, $\rho_{RR}(D)$, $\rho_{NT}(D)$) of positive asymmetry coefficient γ.

In Table 2, the dimensionless coordinates $z_{0\min}$, for which the average value of the difference $S_\rho(z)$ takes its minimum, are presented.

T a b l e 2. Dimensionless coordinates $z_{0\min}$, for which the average value of the difference $S_\rho(z)$ takes its minimum.

$\rho(D)$	$z_{0\min}$	$I(z_{0\min})$	$S(z_{0\min})$	$S(\bar{z}_0)$	$R(\bar{z}_0)_c$
ρ_t	1.40	0.599	0.0011	0.0020	0.0073
ρ_{tl}	1.44	0.581	0.0003	0.0006	0.0032
ρ_G	1.49	0.558	0.0001	0.0005	−0.0007
ρ_r	1.50	0.553	0.0004	0.0011	−0.0030
ρ_{tp}	1.57	0.521	0.0005	0.0020	−0.0064

$\bar{z}_0 = 1.47$, $\quad I(\bar{z}_0) = 0.57$

The average drop diameter $\bar{D}_{\rho s}$ is calculated defining the coordinate $r_{0.55}$ for which $I(r_{0.55}) = 0.55 I_{F\max}$

$$\bar{D}_{\rho s} = \frac{z_{0\min}\lambda f}{\pi r_{0.55}} = 0.47\frac{\lambda f}{r_{0.55}}, \quad \left(\frac{\Delta D}{\bar{D}_{\rho s}} \leqslant 0.1\%\right). \tag{26}$$

The relative error $\Delta D/\bar{D}_{\rho s}$ caused by taking the average value of $z_{0\min}$ instead of $z_0(d)$ is less than 0.1%.

For the distributions of positive asymmetry coefficient γ the zero place $z_{0\min}$ is less than 1.50 ($\rho_{tl}(D) \to z_{0\min} = 1.44$, $\rho_l(D) \to z_{0\min} = 1.40$), while for $\gamma < 0$ the minimum of the function $S_\rho(z)$ is shifted towards the greater values of the dimensionless coordinate ($\rho_{tp}(D) \to z_{0\min} = 1.57$).

If there exist any experimental or theoretical circumstances helpful in determining the type of the function $\rho(D)$ or, at least, the sign of the coefficient γ, then the dimensionless coordinate z_0 (and $I(z_0)$), being in a proper relation to the "center" of the interval $1.40 - 1.57$, i.e., $z_{0\min} = 1.50$, for $\gamma = 0$, may be taken to calculate the average diameter $\bar{D}_\rho$ of the drops.

Which value z_0 should be taken in the situation when there is no available information concerning the dimensional structure of the pulverized stream of the liquid? It should be the average $\bar{z}_0$ minimizing the error for the functions $\rho(D)$ of the opposite signs of the asymmetry coefficient γ.

In Figure 13, the point K is marked at which the lines $S_\rho(z)$ for the distributions $\rho_l(D)$ and $\rho_{tp}(D)$ intersect. A dimensionless coordinate $\bar{z}_0 = 1.47$ corresponds to this point, while $S_{\rho l}(\bar{z}_0) = S_{\rho tp}(\bar{z}_0) = 0.002$. The integral average values $S(\bar{z}_0)$, Tab. 2, for the pulverization spectrum $\rho_{tl}(D)$, $\rho_G(D)$ and $\rho_r(D)$ are significantly less.

To make the estimation of the range of possible deviations from the dimensionless intensity at the characteristic point $I_m(\bar{z}_0) = 0.567$ complete, the greatest difference $R(\bar{z}_0) = I_m(\bar{z}_0) - I_\rho(\bar{z}_0)$ calculated for relative stadard deviation $d_k = 0.40$, is presented in the last column of Tab. 2. Obviously, the extreme values $R(\bar{z}_0)_{\max}$ occur for the "extreme" nonsymmetric functions of the drop size distributions $\rho_l(D)$ (0.0073) and $\rho_{tp}(D)$ (-0.0064), Figs. $11-13$. At the characteristic point $I_m(\bar{z}_0) = 0.567$ the derivative $dz/dI_m = 2.17$ and therefore the limiting estimation errors for the dimensionless coordinate $\bar{z}_0$ amount to $\Delta z_{\rho l} = 0.016$ and $\Delta z_{\rho tp} = -0.014$, respectively, hence $\Delta \bar{z}_\rho / \bar{z}_0 = \pm 1\%$

The final conclusion from the above analysis is that independent of the type of the drop pulverization spectrum $\rho(D)$ and the relative standard deviation d, the abscissa of the point at which the dimensionless light intensity $I(z)/I_{F\max} = 0.57$ cannot differ by more than 1% from the average value $\bar{z}_0 = 1.47$ proper for the monodispersive medium. The relation for the average diameter $\bar{D}_\rho$ of the drops in the pulverized stream of the liquid of unknown quantitative composition $\rho(D)$ differs from formula (26) only by the coefficient

$$\bar{D}_\rho = \frac{\bar{z}_0 \lambda f}{\pi r_{0.57}} = 0.468 \frac{\lambda f}{r_{0.57}}, \quad \left(\frac{\Delta D}{\bar{D}_\rho} \leqslant 1\% \right). \tag{27}$$

The influence of asymmetry of pulverization spectrum γ and the relative standard deviation d on the value of the zero place of the diffrence $R_\rho(z)$ is illustrated by five functions $\rho(D)$, Figs. $11-13$, Tab. 2. The conclusions are formulated by analysing several different statistical distributions (including several histograms based on the results of measurements carried out with the use of other methods for different dispersing agents of the liquid).

The assumption of the upper limit of the relative standard deviation $d_k = 0.40$ when calculating the entire integral average $S_\rho(z)$ can be of slightly arbitrary

character (24). This value is adequate under the circumstances when there appears a relatively large number of drops of dimensions highly exceeding the average diameter $\bar{D}_0$ (*i.e.*, $\gamma > 0$). When the pulverization spectrum $\rho(D)$ is "spread" in the direction of drops of small sizes ($\gamma < 0$), then the influence of the limiting value D_g defined by relation (25) is marked by standard deviation greater than $d_k = 0.40$.

However, it has been stated that 10% magnification of the upper limit d_k of the interval in which the average is calculated from the modulus of the difference $|R(z)|$ causes the change in position of the minimum of the function $S_\rho(z)$ only within the interval $0.05 - 0.50\%$ (depending on the type of distribution function). This has no influence, however, on the dimensionless coordinate of the characteristic point $\bar{z}_0$ since the eventual change of the value d_k causes the shift of curves $S_{\rho l}(D)$ and $S_{\rho t p}(D)$ in the opposite directions and the abscissa of the point K at which they intersect (Fig. 13) will not suffer from change.

The characteristic point of the light intensity distribution $I_F(r)$ diffracted by the aerosol drops the position of which is dependent, in practice, only on the average size $\bar{D}_0$ of the drops can be used for its direct visualization [13].

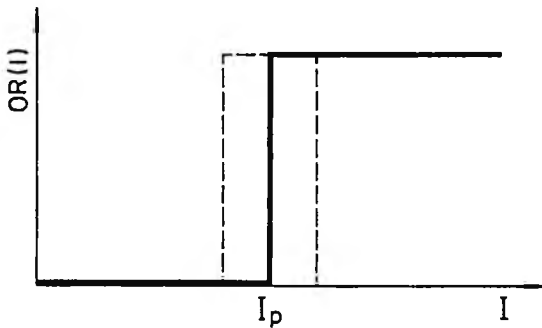

Fig. 14. Transducer of step-like characteristics of the optical response OR(I).

If a transducer of step-like characteristics of the optical response (OR(I) in Fig. 14) is located in the image plane of the objective transforming the plane monochromatic wave passing through the medium under examination, the diffraction image will be reduced to the circle of diameter δ

$$I_F(r) = I_p \to \delta = 2r. \tag{28}$$

Establishing the threshold intensity of the transducer at the level of

$$I_p = 0.57 I_{F\max} \to \delta = 2r_{0.57} \tag{29}$$

the visualisation of the coordinate $r_{0.57}$ is made (Fig. 15). The value of the average drop diameter $\bar{D}_\rho$ can be read out directly from the scale introduced on the basis of relation (27). The intensity $I_{F\max}$ of the diffraction part of the entire light intensity distribution $I(r) = I_0(r) + I_F(r)$ appearing in the image plane is proportional to the number of drops located in the space in which the monochromatic plane wave propagates. Condition (29) will always be fulfilled if the threshold value changes also proportionally to the number of drops causing the diffraction of the light wave.
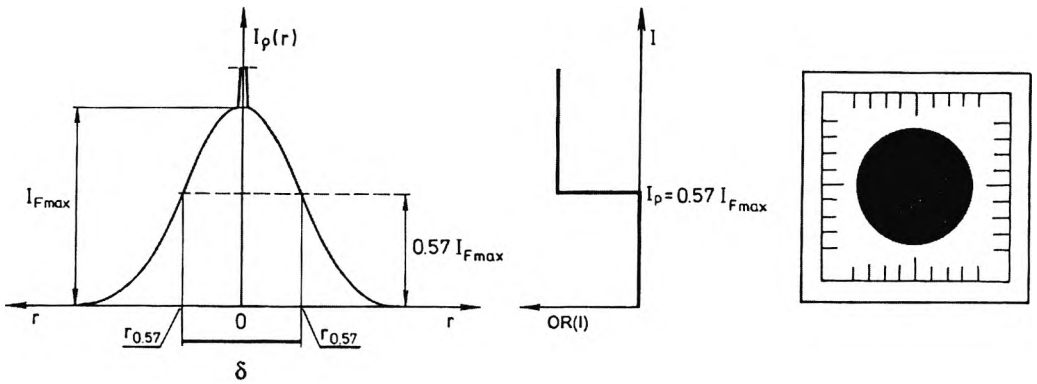
Fig. 15. Scheme of transducing the light intensity distribution $I_p(r)$ into an image of diameter $\delta = 2r_{0.57}$.

In Figure 16, a conceptual scheme of an optical system in which the optical transducer is controlled by a signal from detector measuring the diffraction image intensity $I_{F\max}$ is shown. The limited sizes of the active area of the transducer and hyperbolic character of the dependence between the average diameter $\bar{D}_p$ of the drops and the coordinate of the characteristic point $r_{0.57}$ cause the width of the measurement range $(D_p - D_k)$ to be defined by the relation $D_k \approx 2D_p$. Optimization
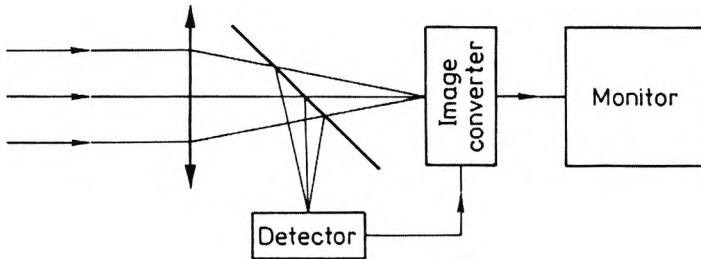

Fig. 16. Conceptual scheme of the measuring system to direct measurement of the average diameter $\bar{D}_p$ of the aerosol drops.

of the geometric parameters of the measurement line is possible practically only by choosing the focal length f of the objective transforming the diffraction image $I(r)$ of the aerosol stream under test. The reduced diameter of this image $\delta = 2r_{0.57}$ cannot be greater than the linear dimension l_p of the transducer.

The maximum value of the focal length f is defined by the condition

$$\delta \leqslant l_p \to f \leqslant \frac{l_p}{2} \frac{D_p}{0.468\lambda} \simeq \frac{D_p l_p}{\lambda}. \tag{30}$$

In Figure 17, an exemple of scale $D(r_{0.57})$ adjusted to the measurement range $D = 12 - 24$ μm and the image converter of size $l_p = 30$ mm is shown. From condition (30) it follows that for the wavelength $\lambda = 0.63$ μm the focal length
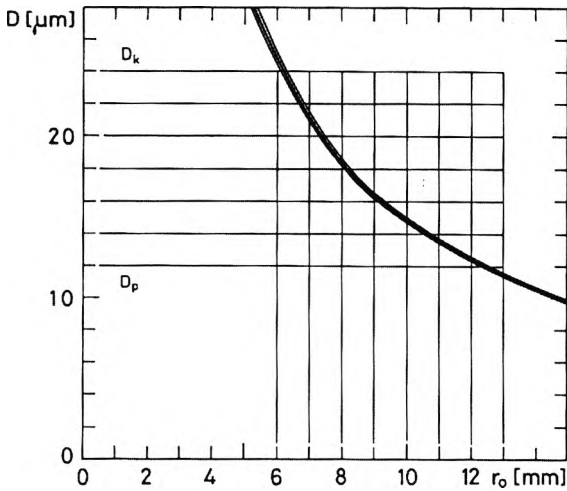
Fig. 17. Dependence of the average diameter $\bar{D}_p$ of the drops on the coordinate $r_{0.57}$ ($l_p = 30$ mm, $f = 500$ mm, $\lambda = 0.63$ μm).

$f \leqslant 0.61$ m, and therefore the typical value $f = 0.5$ m has been accepted. The extreme lines $D(r_{0.57})$ illustrate the limiting systematic error caused by averaging the coordinates of zero places $z_0(d)$ of the function $R_p(z)$.

The scale presented in Fig. 17 renders it possible to read out the drop sizes with the accuracy which is approximately the same in the whole range $(D_p - D_k)$. The criterion of the constant error is satisfied up to the level $D_k = D(r_{\min})$ while $r_{\min} \approx \delta/6$. For $r < r_{\min}$ the measurement of the diameter $\bar{D}_p$ is still possible but with less accuracy. The dependence $D(r_{0.57})$ is "steeper" in this region and therefore even the slight changes of the radius Δr of the transduced diffraction image cause significant differences when reading out the value $\bar{D}_p$.

The trials carried out on the prototype measuring stands confirmed the possibility of direct measurement of the average diameter $\bar{D}_p$ of the drops. On this basis the practical estimation of the "capacity" of this method has been made from which it follows that it is defined by the relation $D_k \approx 2D_p$ for a single objective. This means that in order to widen the measurement range a set of parafocal objectives of focal lengths forming a series of sizes: f, $2f$, $4f$ ... is necessary.

The step-like characteristics of the optical response OR(I) can be obtained by suitable steering of the TV camera and employing optoelectronic transducers of the image.

The threshold effects characteristic of ordered layers of liquid crystal appeared to be exceptionally useful due to the ease of steering the threshold position l_p and high contrast at the rim of the transduced light intensity distribution $I_p(r)$, [14], [15].

The most important advantage of this version of diffraction method is a possibility of determining the substitute diameter $\bar{D}_p = D_{10}$ in the course of measure-

ment by direct readout from the scale. This property is especially important in the diagnostics, *i.e.*, when estimating the degree of pulverization of the fuel for the whole series of pulverizing devices of the same type.

7. Comparison of methods determining the average drop diameter $\bar{D}_\rho$ from the light intensity distribution $I(r)$ in the diffraction image

The analytic methods allowing us to determine the average diameter $\bar{D}_\rho$ of the aerosol drops on the basis of light intensity distribution $I(r)$ differ by the way the information contained in the diffraction image is transduced.

The measurement of the position of dark and bright rings appearing after Fourier transformation the light wave propagating through the pulverized stream of the liquid renders it possible calculate of $\bar{D}_\rho$ from the classical formulae. This is the simplest variant due to the way the image appearing in the focal plane is recorded. The position of the extrema of the light intensity distributiom $I(r_i)$ is the source of information about the drop sizes which allows the photographic techniques to be applied to its recording. The measurement range of this variant of the diffractive method is limited to the quasi-monodispersive media for which the relative standard deviation of the pulverization characteristics $\rho(D)$ does not exceed $d_q = 0.153$.

The analysis of the images created by aerosol of significant diversification of the drop sizes is more complex and possible only when the absolute values of the light intensity distribution $I(r)$ are known. The approximation of the quasi-linear fragment of the dependence $I(r)$, Fig. 2, means the exploitation of only $\sim 1/4$ of the information contained in the diffractogram (Fig. 18, fragment B).
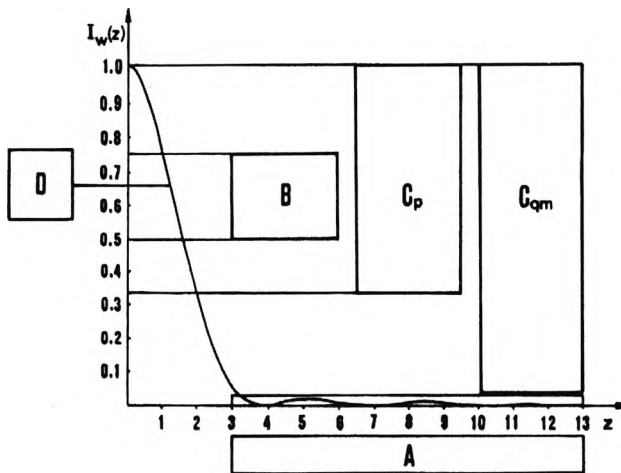

Fig. 18. Range of information transduced from the light intensity distribution $I_w(z)$. A — method taking advantage of the position of the diffraction fringes, B — method of liner approximation of the distribution $I_w(z)$, C_p, C_{qm} — method of linear transformation of the light intensity $I_w(z)$, D — method of visualisation of the characteristic point z_0.

Linear transformation of the distribution $I(r)$ (Tab. 1) allows us to calculate the average drop diameter $\bar{D}_\rho$ based on the data from the broadest interval of the dimensionless light intensity since $I_w(r) = 0.33 - 1$ (for polydispersive media — Fig. 18, fragment C_p) and $I_w(r) = I(r_{0.5}) - 1$ (for quasi-monodispersive media, Figs. 9 and 18, fragment C_{qm}).

The measurement of the drop diameter $\bar{D}_\rho$ can be made taking advantage of the point $I_w(r_{0.57}) = 0.57$ and relation (27). This point is characterized by the fact that its position is independent of pulverization spectrum $\rho(D)$ and the relative standard deviation d.

The amount of data about the light intensity distribution $I(r)$ in the diffraction image used to determine the average diameter $\bar{D}_\rho$ of aerosol drops has a direct influence on accuracy of the results obtained.

The least (systematic) error is characteristic of the method of linear transformation of the dimensionless function $I_w(r) = I(r)/I_{F\,max}$ (Fig. 7). It should be emphasized, however, that it is possible to acquire the experimental data (in practice) only after having automatized the measurements and applying numerical calculation procedures.

Taking advantage of the quasi-linear character of the changes in light intensity distribution $I(r)$ leads to significantly simpler calculation formulae and is a basis for the graphic method allowing us to obtain quickly the preliminary results. The restricted range in which the approximation of the relation $I_w(r)$ can be obtained (Fig. 18, fragment C) causes the results to be charged with an error twice as big as that of the linear transformation method. This error is further increased when the diffraction image is recorded with a photographic technique. This is due to the limitations characteristic of the process of reconstruction of the light intensity distribution $I'(r)$ from the microdensitogram $\Phi(r)$.

The determination of the coordinate r_0 of the characteristic point $I_w(r_0) = 0.57$ and calculation of the average diameter from relation (27) can be formally treated as the reduced form of the linear transformation method in which the slope of the transform $z = t(r)$ is determined based on two points (r, z), i.e., $(0, 0)$ and $(r_{0.57}, 1.464)$, Tab. 1. Substituting the value $\tan \gamma = 1.464/r_{0.57}$ to formula (19) formula (27) is obtained.

It should also be emphasized that the dimensionless coordinate z_0 is located in the vicinity of the extremum of the derivative dI_w/dz, which means that even small changes in the average drops diameter $\bar{D}_\rho$ cause a significant increase (or decrease) of the light intensity $I_w(z)$ in the diffraction image. A good conditioning of the point $I_w(z_0)$ causes the accuracy of evaluation of $\tan \gamma$ to be only two–three times less than that which could be achieved by linearly transforming the dependence $I_w(z)$. The greatest advantage following from the metrological properties of the characteristic radius $r_{0.57}$ is the possibility of designing an automatic device for continuous visualisation of the average diameter $\bar{D}_\rho(t)$ of the drops appearing within the region of light wave propagation.

The classical method is convenient in applications due to the fact that no linearity of the relation between the light intensity in the stream image $I(r)$ and the

diffractogram is required to determine the position of diffraction rings. This makes it possible to take advantage of the photographic recording and omit the tedious process of transforming data from the microdensitgram $\Phi(r)$ into a proportional dependence $I'(r)$. This method is very efficient when determining the average sizes of objects characterized by inconsiderable size variability. However, for these reasons this method is of marginal significance in the metrology of fuel aerosols which are typical polydispersive media. From many examined pulverising devices applied in the aircraft turbine engines only the starting injectors (of fuel discharge $Q(p) < 10$ l/h) appear to produce streams of properties of quasi-monodispersive systems.

In the aforesaid measurement methods used to determine the average drop diameter $\bar{D}_p$ the different fragments of the dimensionless light intensity $I_w(z)$ are exploited (Fig. 18). The magnitude of the observed image $I(r)$ is inversely proportional to the value $\bar{D}_p$ being proportional to the focal length f of the objective Fourier transforming the light wave passed through the pulverized stream of liquid. The proper choice of the parameters of the measuring line consists in letting this part of the distribution $I(r)$, which is necessary to realise the chosen variant of the diffraction method, to be placed in the recording plane.

The maximal radius r_p of the active area of the image recording system (or the length of the scanning line l_p) is usually of constant value characteristic of the type of detecting device applied. The optimal exploitation of this area is possible if the focal length f remains in a suitable relation to its sizes. Figure 19 shows the dependence of the dimensionless parameter $\bar{D}/\lambda$ on the quotient f/r_p for four basic variants of the diffraction method enabling determination of the relation between the
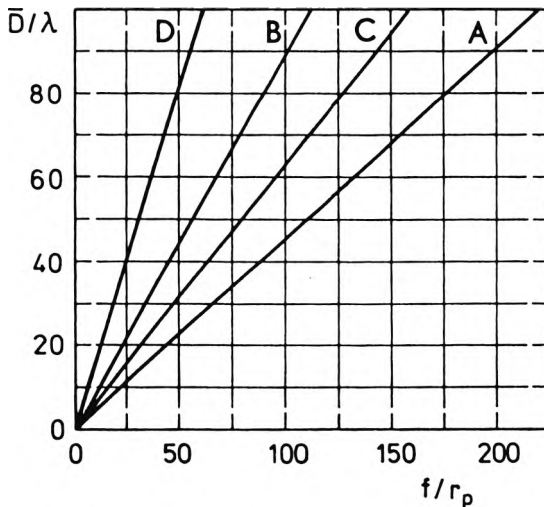

Fig. 19. Choice of the focal distance f of the objective transforming the diffraction image of the aerosol stream of average diameter $\bar{D}$ into the recording system of the radius r_p, (A — method exploiting the position of the diffraction rings, B — linear approximation method of the light intensities distribution $I_w(z)$, C — linear transformation method of light intensity $I_w(z)$, D — method of visualization of the characteristic point z_0).

radius of the active area r_p, the focal length f, the wavelength λ and the foreseen average diameter $\bar{D}_p$.

The model of single scattering of the light by the aerosol drops has been assumed. When the multiple-scattering occurs and there is no possibility of limiting mechanically the pulverization cone the results of the measurement are charged with a systematic error difficult to estimate. Therefore, the following question arises: is it possible to modify the calculation formulae (8), (12), (15), (19), (26) and (27) in such a situation? These relations can be readjusted to a more complex model of light scattering though to a degree different for particular variants of the diffraction method. It is most difficult to achieve this in the case of calculating the average drop diameters $\bar{D}_p$ from the position of extrema of light intensity $I(r_i)$, which is caused to some degree by limited range of the way the data from the diffraction image are processed. The most universal and "open" is the linear transformation method. If the effects of multiple-scattering of the light waves by the drop of the aerosol examined, their mutual interaction, Van de Hulst scattering effect and the like are taken into account the "construction" of this method remains unchanged being reduced only to the correction of the data from the transformation Table 1.

References

[1] OPARA T., *Metrology Aspects of Phenomena Investigation Arising in the Turbojets Spraying Cone* (in Polish), WAT, Warszawa 1996.

[2] OPARA T., *Diffraction method for drop size measurement in polydispersive aerosol, I, Photographic recording of light intensity distribution in diffraction picture*, Biul. WAT (in Polish), **43** (1994), 135.

[3] HIRLEMAN E.D., *Optimal scaling of the inverse Fraunhofer diffraction particle sizing problem: analytic eigenfunction expansions*, [In] Proc. European Symposium: Particle Characterization, Nürnberg 1989, p. 339−345.

[4] HIRLEMAN E.D., *Optimal scaling of the inverse Fraunhofer diffraction particle sizing problem: the linear system produced by quadrature*, Part. Charact. **4** (1987), 128.

[5] MROCZKA J., J. Aerosol Sci. 20 (1989), 1075.

[6] MROCZKA J., Opt. Commun. **99** (1993), 147.

[7] MROCZKA J., *Metrological aspects of integral solution applications in the ensamble method of particle sizing*, [In] Proc. Conf. *Optical Diagnostics in Fluid and Thermal Flow*, July 14−16, 1993, San Diego, U.S.A., Proc. SPIE **2005** (1993), 387.

[8] JANKOWSKA-KUCHTA E., *Diffraction method of the burners fuel atomization quality assessment*, Silniki Spalinowe, No. 2−3 (19860), 65, (in Polish).

[9] GNIADEK K., *Optical Processing Information*, (in Polish), WNT, Warszawa 1992.

[10] MEYER-ARENDT J.R., *Introduction to Optics* (in Polish), PWN, Warszawa 1977.

[11] OPARA T., Biul. WAT, **43** (1994), 147 (in Polish).

[12] EADIE W.T., DRIJARD D., JAMES F.E., SADOULET B., *Statistical Methods in Experimental Physics*, (in Polish), PWN, Warszawa 1989.

[13] OPARA T., Biul. WAT **43** (1994), 155. (in Polish).

[14] ADAMCZYK A., STRUGALSKI Z., *Liquid Crystals*, (in Polish), Warszawa 1976.

[15] ADAMCZYK A., *Unusual Matter State. Liquid Crystals* (in Polish), WP, Warszawa 1981.